Available online at www.sciencedirect.com
ScienceDirect
Journal of Power Sources 175 (2008) 175–182
JOURNAL OF POWER SOURCES
www.elsevier.com/locate/jpowsour

Preparation, characterization, and high performance of RuSe/C for direct methanol fuel cells

Alexey Alexandrovich Serov, Myoungki Min, Geunseok Chai, Sangil Han, Soonki Kang, Chan Kwak *

Corporate R&D Center, Samsung SDI, Shin-dong 575, Yeongtong-gu, Suwon-si, Gyeonggi-do 443-731, South Korea

Received 3 June 2007; received in revised form 24 August 2007; accepted 30 August 2007
Available online 4 September 2007

Abstract

RuSe/C catalysts prepared by different methods have been tested for oxygen reduction and the results analyzed based on the active species and particle size distribution. Inorganic precursor methods exhibit higher catalytic performance than the carbonyl method. Selenious acid is an excellent inorganic precursor. X-ray photoelectron spectra indicate that selenium in a high oxidation state is more active than that with zero valence. The effect of operating conditions is analyzed for catalysts prepared by the inorganic precursor method. The optimum heat-treatment temperature for both active phase formation and particle size distribution is 300 °C. A performance of 62 mW cm^{-2} at 80 °C is obtained using 80 wt.% RuSe/C in the cathode.

Keywords: Ruthenium; Selenium; Fuel cell; Cathode; Catalyst

1. Introduction

Research interest in fuel cells is increasing from year to year. Significant and careful investigations in this field have produced energy-converting devices that are nearly ready to be commercialized. Up to now, all low-temperature fuel cells, such as the polymer electrolyte membrane fuel cell (PEMFC) and the direct methanol fuel cell (DMFC), have used platinum or platinum alloys as the electrode materials. Platinum has the highest catalytic activity and stability; therefore its wide use in most fuel-cell systems is reasonable. On the other hand, its high cost is a problem for successful commercialization. Two ways of reducing the cost of the catalyst have been tried, i.e. low-platinum loading [1,2] and non-platinic catalysts [3–13]. The latter approach of using platinum-free catalysts not only solves the cost problem but also offers additional advantages. A considerable amount of methanol crossover occurs from the anode to the cathode side in general DMFCs, resulting in a mixed potential on the platinum cathode. Sensitivity to admixtures of air, such as sulfur-containing compounds, carbon monoxide, and various nitrogen oxides, is also a significant drawback of platinum electrodes.

At the present level of fuel-cell research, most efforts are being directed towards cathode materials consisting of non-platinic catalysts. Non-platinic oxygen-reduction reaction (ORR) catalysts can be divided into two classes, i.e. derivatives of transition-metal macrocyclic compounds [3–6] and Ru-based catalysts [7–13]. Macrocyclic compounds of transition metals show a high turnover frequency in oxygen reduction, but they have some disadvantages. First, the precursors of metal macrocycles are expensive under existing circumstances, their price being comparable with that of platinum precursors in some cases. Their high carbon content prevents an increase of the metal loading in the macrocyclic catalysts, resulting in a reduction of the overall ORR activity.

Ruthenium chalcogenides [7–13] can be separated into Chevrel phases [7] and amorphous ruthenium chalcogenides [9]. For example, Ru–Mo(W)–S(Se) is as a good candidate for ORR because of electron localization in metal clusters [7]. In the next stage of research, amorphous ruthenium chalcogenides such as Ru_xCh_y (Ch = S, Se) were proposed as promising cathode materials [9,10]. Amorphous catalysts treated at low temperatures show efficient electrocatalytic activity towards ORR in an acidic medium. Amorphous ruthenium chalcogenides have typically

* Corresponding author. Tel.: +82 31 210 7085; fax: +82 31 210 7374.
E-mail address: c.kwak@samsung.com (C. Kwak).

0378-7753/$ – see front matter © 2007 Elsevier B.V. All rights reserved.
doi:10.1016/j.jpowsour.2007.08.089

been prepared from carbonyl precursors [7–11]. However, this method is limited in mass production because of the high cost of the carbonyl precursors, the complicated operation process, and the toxicity of the substances. Recently, different ruthenium and selenium precursors, such as ruthenium oxalate, ruthenium colloids, and selenious acid, have been proposed for the preparation of amorphous ruthenium selenide [12,13].

The present study is particularly concerned with preparation methods using inorganic precursors. A series of such catalysts was prepared, tested for oxygen electroreduction in half-cells as well as in fuel cells, and characterized by X-ray diffraction (XRD), X-ray photoelectron spectroscopy (XPS), and transmission electron microscopy (TEM).

2. Experiment

2.1. Catalyst preparation

A series of RuSe/C catalysts was prepared by three different methods.

2.1.1. Method I

A calculated amount (0.3 g) of selenium powder was dissolved in de-aerated xylene at 140 °C. After cooling the solution to room temperature, $Ru_3(CO)_{12}$ and carbon (Ketjen black) were added successively to the solution, which was being stirred and bubbled with nitrogen. After refluxing at 135 °C for 24 h, the solution was filtered and the obtained black powder was dried in an oven at 80 °C overnight. Heat treatment was performed in a flow of hydrogen.

2.1.2. Method II

$RuCl_3{\cdot}xH_2O$ was deposited on a carbon (Ketjen black) surface by the incipient wetness method with a minimal amount of solvent. The solid was dried in vacuum for 3 h and calcined in hydrogen at 300 °C. The prepared Ru/C was dispersed in hot xylene. Selenium powder was added to the solution. After refluxing at 135 °C for 24 h, the solution was filtered and the obtained black powder was dried at 80 °C overnight. Heat treatment was performed in a flow of hydrogen.

2.1.3. Method III

The first stage of Ru/C synthesis was the same as that in Method II. Selenious acid was added by drops to the Ru/C, which was then dried in vacuum followed by heat treatment in a flow of hydrogen.

All of the catalysts contained around 32 wt.% ruthenium. The real content of ruthenium in the catalysts prepared by Methods II and III was the same as the nominal content, because there was no filtration process in these methods. In Method I, the ruthenium content was controlled by changing the solution concentration and weighing the mass of reduced powder. Some selenium was lost during the heat treatment. The selenium content measured by energy-dispersive X-ray analysis (EDAX) is shown in Table 1. The selenium content is indicated in the form of a range, because each point shows a slightly different value.

Table 1
Content of RuSe/C from EDAX analyses

Method	Heat treating temperature (°C)	Nominal atomic content, Se/(Se + Ru)	Atomic content from EDAX, Se/(Se + Ru)
I	300	10	3–5
II	300	5	3–4
II	300	10	5–6
II	300	15	6–8
III	250	10	5–6
III	300	5	3–4
III	300	10	5–6
III	300	15	6–8
III	350	10	4–5

2.2. Rotating disk electrode

The oxygen-reduction reaction on the prepared RuSe/C electrocatalyst was studied using a rotating disk electrode. Working electrodes were prepared by mixing 11 mg of the RuSe/C electrocatalyst, 1.13 ml of water, and 1.13 ml of isopropyl alcohol. The mixture was sonicated before a small volume (13.1 μl) was applied onto a glassy carbon disk with a sectional area of 0.283 cm^2. After drying the droplet, at room temperature, 11.2 μl of a Nafion® monomer solution (0.5 wt.%, Dupont) was applied onto the film. The loading of metal on the electrode was 0.225 mg cm^{-2}. The experimental setup involved a three-electrode arrangement connected to a potentiostat/galvanostat (Autolab model PGSTAT30). The reference electrode was Ag/AgCl and the counter-electrode was a platinum mesh. The electrochemical reduction reactions were performed by rotating the catalyst-loaded electrodes at 2000 rpm at a scan rate of 10 mV s^{-1} in 50 ml of 0.5 M H_2SO_4 at 25 °C.

2.3. Characterization

X-ray diffraction (XRD) analysis of the catalysts was carried out employing a Philips X'pert diffractometer (Cu Kα radiation). The diffractogramms were identified using the JCPDS database.

X-ray photoelectron spectroscopy (XPS) measurements were performed with an ESCALAB250 (VG Scientific, England) system using monochromatic Al Kα radiation (1486.6 eV). Powder samples were mounted on pre-cleaned indium foils.

Samples for transmission electron microscopy (TEM) were prepared by grinding and successive ultrasonic treatment in isopropyl alcohol for 1 min. A drop of the suspension was dried on a standard TEM sample grid covered with holey carbon film. Tecnai™ G^2TEM with FEG was used for observations. Images were recorded with a Multiscan camera.

2.4. Single cell test

The membrane electrode assemblies (MEAs) were fabricated by spraying the catalyst ink onto Nafion® 112. The anode catalyst is PtRu black (Johnson Matthey, 4.1 mg cm^{-2}) and the cathode catalysts are 32 and 80 wt.% RuSe/C (5.9 and 7.1 mg cm^{-2}). The Nafion® content in the anode is 15 wt.%. The Nafion® contents in the cathode are 40 wt.% for 32 wt.%

RuSe/C, and 30 wt.% for 80 wt.% RuSe/C. The catalyst-coated membrane was sandwiched between the anode gas diffusion layer (GDL, SGL 10AC) and the cathode GDL (SGL 31BC) and then the assemblies were hot-pressed under a specific load of 140 kgf cm^{-2} for 3 min at 125 °C.

Polarization curves were obtained by the Wonatech testing system using a homemade single cell with a working area of 10 cm^2. Methanol solution (1 M) was fed to the anode side of the cell (anode stoichiometry = 3) while dry air was fed to the cathode side (cathode stoichiometry = 3) under atmospheric pressure. The single cell operated at 80 °C.

3. Results

3.1. X-ray diffraction

Fig. 1 shows the wide-angle XRD patterns of catalysts prepared by Method III calcined at different temperatures. Six peaks positioned at $2\theta = 38.4°$, 44.0°, 58.5°, 69.5°, 78.5°, and 85.2° correspond to the lattice planes of the ruthenium metal. A peak at 25.1° is characteristic of amorphous carbon from the Ketjen black support. Selenium or selenide phase is not detected in the diffractogram, indicating either that all the selenium is present in the form of a fully amorphous phase or that the amount of crystalline selenium phase is below the XRD sensitivity. It has been reported that no stoichiometric compound of RuSe is present in semi-amorphous ruthenium selenide catalysts [10].

3.2. TEM

The representative TEM images of catalysts prepared by Methods II and III, shown in Fig. 2(b) and (c), reveal that

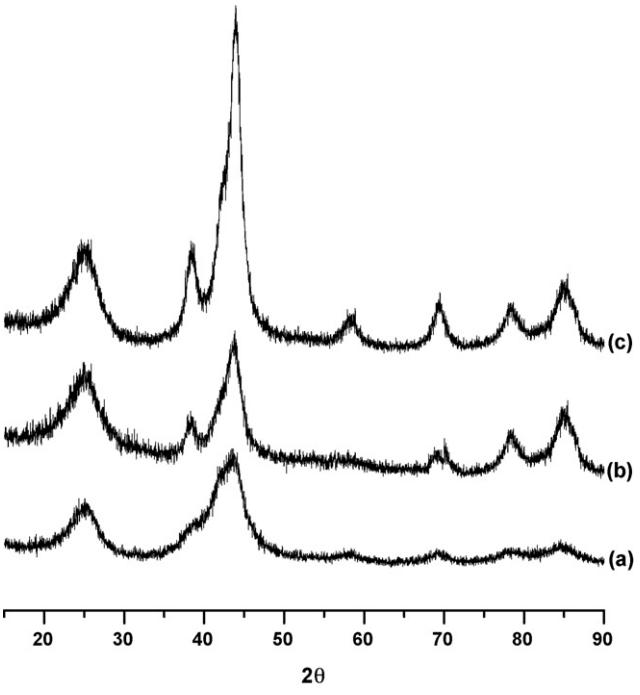

Fig. 1. X-ray diffractograms of Method III catalysts containing 10 at.% selenium calcined at (a) 250 °C, (b) 300 °C, and (c) 350 °C.

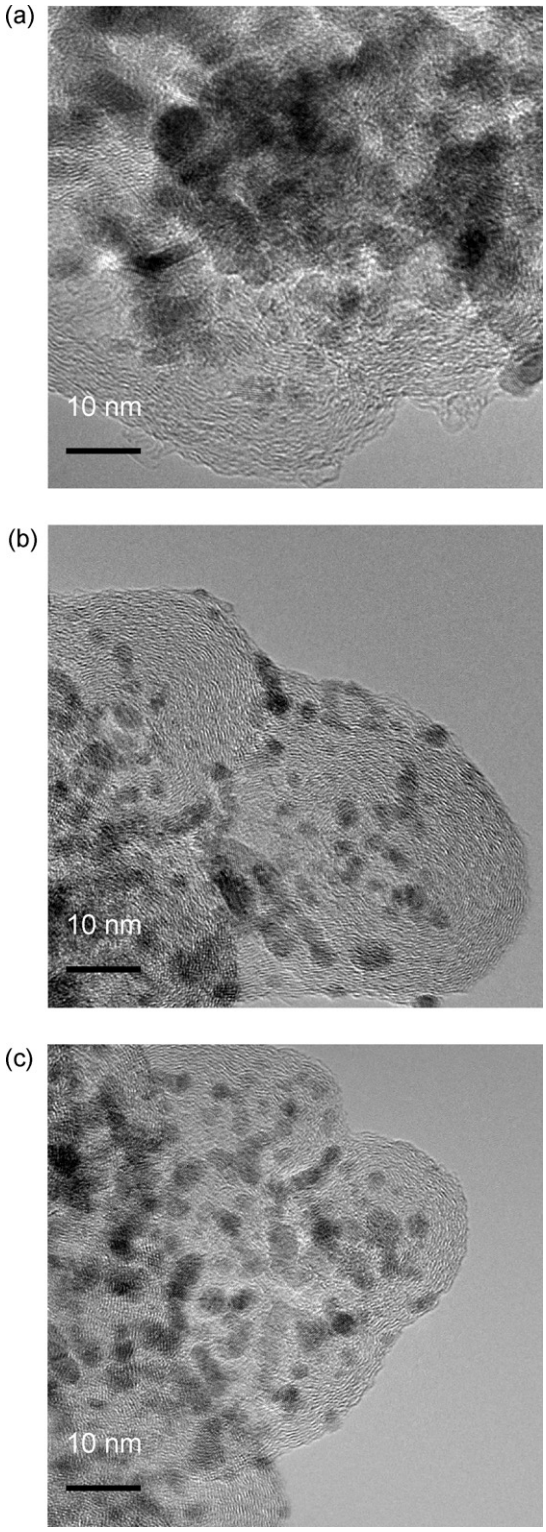

Fig. 2. TEM images of RuSe/C prepared by (a) Method I, (b) Method II, and (c) Method III. The selenium content was 10 at.% and the calcination temperature 300 °C.

3–4 nm ruthenium particles are uniformly dispersed in the carbon support. In contrast, the catalyst prepared by Method I has agglomerated regions with larger particles, as shown in Fig. 2(a).

The temperature dependence of the particle size is shown in Fig. 3. The average particle size of the sample treated at 250 °C

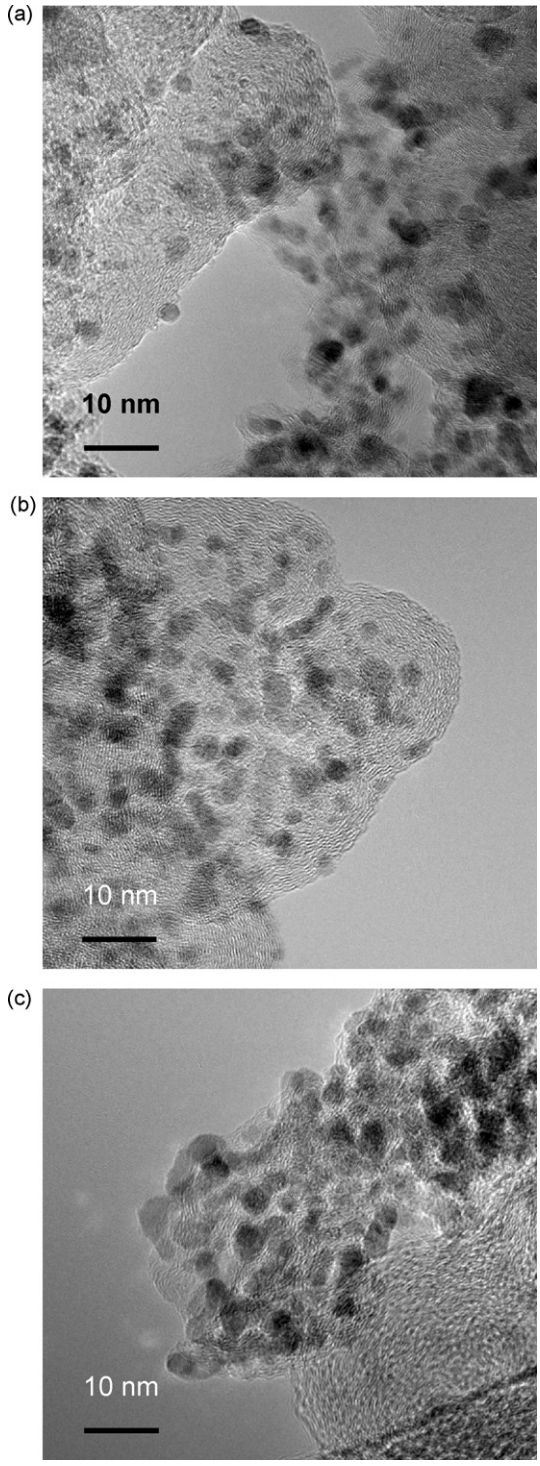

Fig. 3. TEM images of Method III catalysts containing 10 at.% selenium calcined at (a) 250 °C, (b) 300 °C, and (c) 350 °C.

is about 2–3 nm, while it is 3–4 nm for the sample treated at 350 °C. It should be noted that the sample calcined at 350 °C has a high level of crystallinity and some agglomerated particles. This dependence is in good agreement with the X-ray diffraction results at different calcination temperatures.

Two periods of calcinations took place during the procedures of Methods II and III. The first calcination was performed after the deposition of ruthenium at low temperature, followed by a second calcination after selenium addition at higher temperatures. Therefore, further aggregation of ruthenium particles can occur during the second calcination step after the addition of selenium. As shown in Fig. 4, the nature of the selenium precursor has only a very slight effect on the particle size of the final state. The influence of the selenium content on the ruthenium particle size is also small.

3.3. XPS

The XP spectra of selenium measured for the catalysts prepared by different methods are presented in Fig. 5. The binding-energy values for the Se 3d peak appear at about 55.0 and 58.5–58.8 eV. The low-binding-energy peak could be assigned to the presence of the selenium species in a high oxidation state, while the other peak is due to the presence of a selenium species with zero valence [14,15]. The latter species can be defined as elemental selenium on carbon or selenium interacting only with ruthenium. The high-binding-energy peak changes its position slightly (±0.2) as a function of the preparation method, suggesting that the kind of selenium in a high oxidation state is different.

The catalyst prepared by Method I shows only one low-intensity peak at 58.6 eV (curve a, Fig. 5). There are two reasons for this. First, the amount of selenium on the ruthenium surface is small in this sample. Secondly, most of the selenium is interacting with a strong anion, i.e. oxygen from the carbonyl group, so elemental selenium or selenium interacting with ruthenium is not present on the surface of the ruthenium. Methods II and III show two peaks in both regions (curves b and c, Fig. 5); however, their relative intensities are different depending on the type of selenium precursor. Selenious acid produces a larger amount of selenium species in a high oxidation state than elemental selenium.

The effect of the heat-treatment temperature on the Se 3d spectra is presented in Fig. 6. With increasing heat-treatment temperature, a distinct change is observed in the Se 3d band of the RuSe/C prepared by Method III. The low-energy peak is enhanced accompanied by a lowering of the high-energy peak. The above change in the Se 3d bands is due to the decomposition of selenious acid followed by the reduction of selenious oxides on the ruthenium surface.

3.4. Rotating disk electrode

The oxygen-reduction activities of the prepared catalysts were measured by a rotating disk electrode (RDE) and are presented in Figs. 7–9. In order to prevent the ruthenium from dissolving, the measurement was started from 0.78 V. All of the prepared catalysts exhibit an oxygen-reduction current from the initial potential. The electrochemical reaction seems to be mainly under kinetic control in the potential range 0.78–0.6 V. A limiting diffusion current is nearly reached at a cathodic potential of 0.5 V/normal hydrogen electrode (NHE) for the catalysts.

Fig. 7 compares RuSe/C prepared by different methods with Ru/C. The oxygen-reduction activity of Ru/C is much lower than

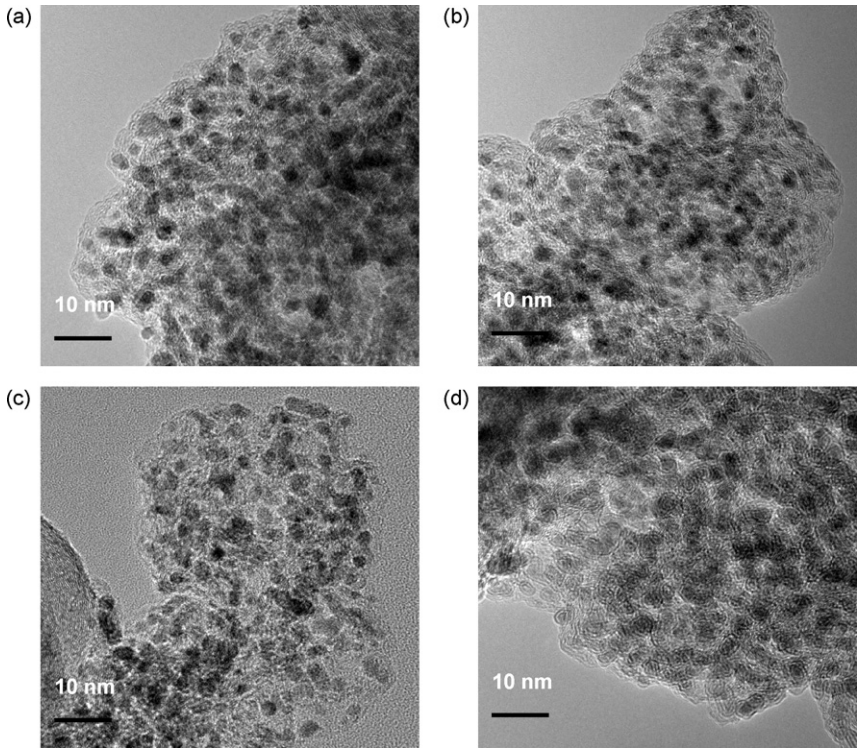

Fig. 4. TEM images of RuSe/C calcined at 300 °C with different selenium contents: (a) Method II, 5 at.% selenium; (b) Method II, 15 at.% selenium; (c) Method III, 5 at.% selenium; and (d) Method III, 15 at.% selenium.

that of the catalysts modified by selenium. The activity of Se/C for oxygen reduction is nearly zero. The inorganic precursor methods (Methods II and III) show much higher catalytic performance than the conventional carbonyl method (Method I). Comparing the precursors of Methods II and III, selenious acid provides more active species than elemental selenium. The heat-treatment temperature affects the catalytic performance to a large extent in Method III, as shown in Fig. 8. The highest catalytic activity is observed with the catalyst calcined at 300 °C due to the combined effect of particle size and formation of active species. The dependence of the catalytic activity on the selenium content in Method III is shown in Fig. 9. The oxygen-reduction activity increases slightly with increasing nominal selenium content.

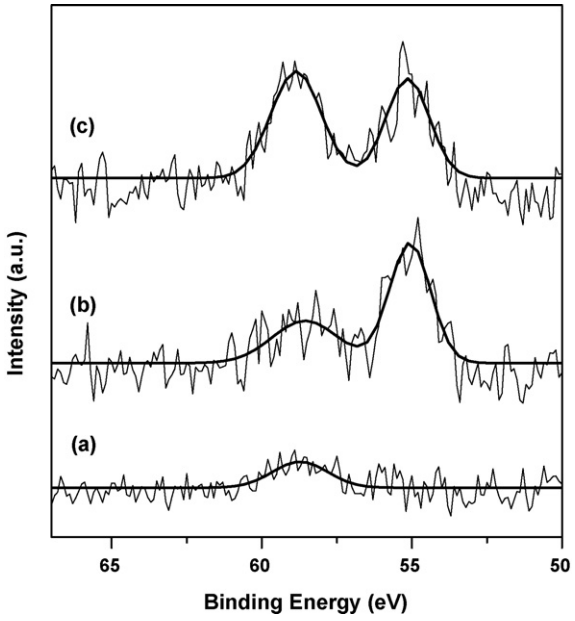

Fig. 5. XP spectra of Se 3d for RuSe/C prepared by (a) Method I, (b) Method II, and (c) Method III. The selenium content was 10 at.% and the calcination temperature 300 °C.

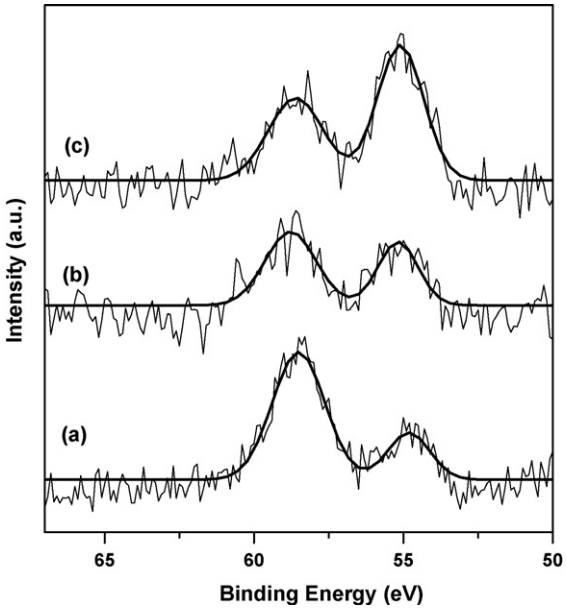

Fig. 6. XP spectra of Se 3d for RuSe/C prepared by Method III calcined at (a) 250 °C, (b) 300 °C, and (c) 350 °C.

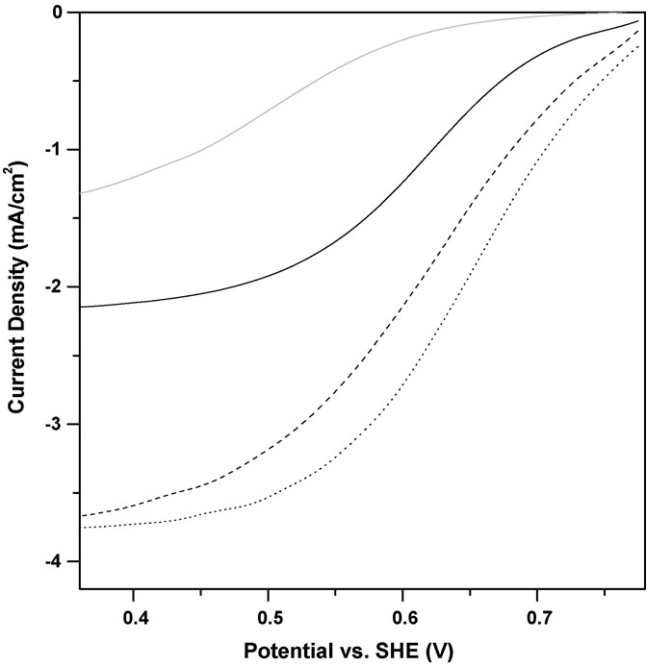

Fig. 7. Steady-state polarization curves for oxygen reduction in 0.5 mol l^{-1} H_2SO_4 solution on a RDE prepared with Ru/C (gray) and RuSe/C from Method I (solid), Method II (dash), and Method III (dot). The selenium content was 10 at.% and the calcination temperature 300 °C.

3.5. MEA performance

Fig. 10 shows the single-cell performance of RuSe/C made by Method III. In order to increase the metal loading in the cathode, 80 wt.% RuSe/C was prepared and its MEA performance is also presented in Fig. 10. The 80 wt.% RuSe/C increased the metal loading of the cathode from 5.9 to 7.1 mg cm^{-2}. The open-circuit voltage (OCV) of the fuel cell is around 0.77 V for both MEAs. As shown in Fig. 10, the cell prepared using 80 wt.% RuSe/C achieves a peak power density of 62 mW cm^{-2}, whereas the cell with low-metal loading in the cathode shows 26 mW cm^{-2} at 80 °C. The higher single-cell performance of 80 wt.% RuSe/C is due to the higher metal loading within the limited space of the effective volume in the MEA.

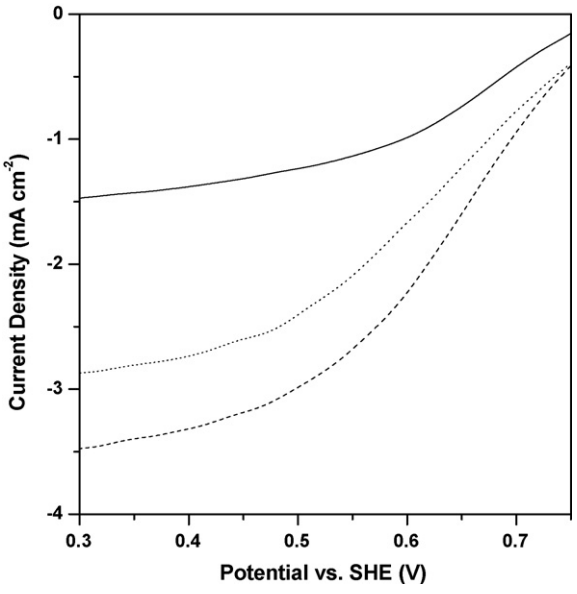

Fig. 8. Steady-state polarization curves for oxygen reduction in 0.5 mol l^{-1} H_2SO_4 solution on a RDE prepared with RuSe/C calcined at 250 °C (solid), 300 °C (dash), and 350 °C (dot). Method III and 10 at.% selenium.

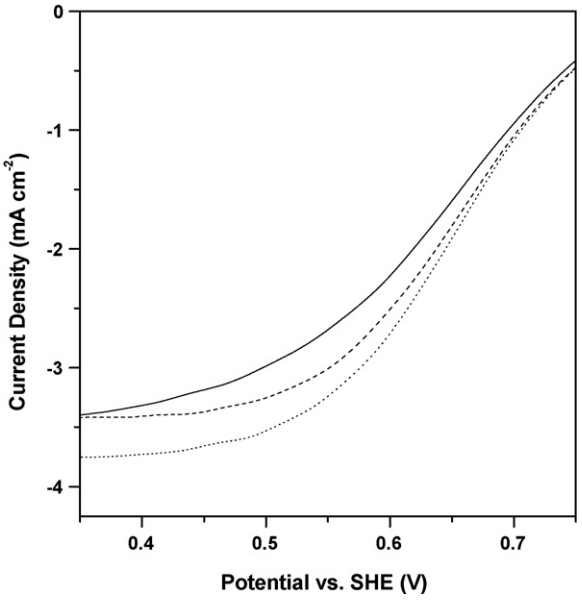

Fig. 9. Steady-state polarization curves for oxygen reduction in 0.5 mol l^{-1} H_2SO_4 solution on a RDE prepared with RuSe/C containing 5 (solid), 10 (dash), and 15 (dot) at.% selenium. Method III and calcination temperature of 300 °C.

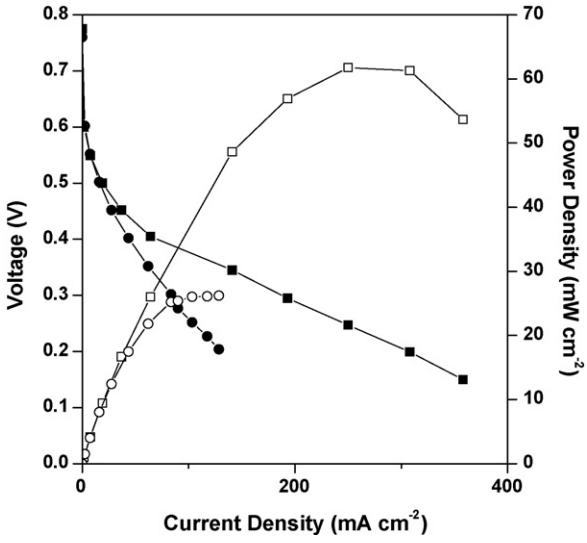

Fig. 10. The polarization curves and power density curves of single cells with 32 wt.% RuSe/C (square) and 80 wt.% RuSe/C (circle). Fuel: 1 M methanol (stoichiometry = 3); oxidant: air under atmospheric pressure (stoichiometry = 3); temperature: 80 °C.

4. Discussion

4.1. Inorganic precursor method

While Chevrel-phase structures containing ruthenium are well known, the structures of amorphous ruthenium selenides

are not clear. The enhancement of the catalytic activity of ruthenium by the addition of selenium suggests that the ruthenium surface is modified by selenium. The XP spectra of selenium suggest that no elemental selenium is present on the surface of the catalyst prepared by Method I. However, the presence of elemental selenium is not clarified in the catalysts prepared by Methods II and III, because the peak position of elemental selenium on carbon is similar to that of selenium interacting only with ruthenium. It is generally accepted that selenium modifies the surface of ruthenium without forming a homogeneous phase [16].

The active species of the catalysts prepared by different methods can be deduced from the XP spectra (Fig. 5). Method I only produces a small amount of selenium species interacting with the strong anion, i.e. oxygen. There are two reasons for the presence of a small amount of surface selenium species on the RuSe/C prepared by Method I. During the preparation procedure of Method I, selenium was added to the solution containing the ruthenium carbonyl before forming ruthenium-metal particles; accordingly, some of the selenium could be distributed inside the ruthenium particles. Another reason is the loss of selenium during the filtration process of Method I. In any case, this selenium interacting with oxygen composes the active phase in the catalyst prepared by Method I. The active species of this catalyst contains carbonyl ligands because the final heat-treatment temperature is not high enough to decompose the carbonyl ligands completely. In the case of sulfur-containing ruthenium, FT-IR spectroscopy has shown that the $Ru_xS_y(CO)_n$ cluster is the active species when it is treated at 300 °C [17].

XP spectra of RuSe/C prepared by Methods II and III show two peaks, representing selenium interacting with oxygen and zero-valence selenium, respectively. It can be supposed that selenium in a high oxidation state constitutes an active phase, as in the case for Method I. The oxygen interacting with the selenium originates from the air in the catalyst prepared by Method II. During the procedure of Method II, elemental selenium was added to reduced ruthenium on carbon, therefore there is no oxygen source other than the air. The surface of the ruthenium is partially oxidized when it is exposed to air. In the case of Method III, a larger amount of selenium in a high oxidation state is observed than in the case of Method II. This phenomenon is caused by the stronger interaction between surface oxygen and selenious acid on the catalyst surface than the interaction of oxygen with elemental selenium. Another reason is that part of the oxygen may originate from the selenious acid precursor. From the XPS and RDE results, it is concluded that the RuSeO phase with selenium in a high oxidation state is more active than the phase with zero-valence selenium.

Bron et al. [10,13,14] have suggested several possible reasons for the positive effects of selenium, i.e. protection of the ruthenium surface from oxidation, improved electrical conductivity due to the electron-conducting role of selenium, and a change of distribution of the interfacial electronic states. With regard to the active species, a ruthenium–carbido–carbonyl complex has been suggested for the carbonyl method [10] and $RuSe_x$ or $RuSe_xO_y$ for the selenious acid method [14].

The catalysts prepared by inorganic precursor methods show higher oxygen-reduction activity than the catalyst prepared by the carbonyl precursor method, as shown in Fig. 7. One possible reason for this is the different active species as described above. However, a more important reason for their better performance than the catalysts prepared by the inorganic precursor methods is the smaller particle size. Methods II and III produce catalysts with smaller particles and better particle distribution in comparison with Method I, as shown by the TEM pictures (Fig. 2).

The nature of the selenium precursor affects the oxygen-reduction activity in the inorganic precursor methods. Selenious acid produces a larger amount of RuSeO phase than selenium powder (see Fig. 5), resulting in higher catalytic activity. The particle size nearly remains unchanged by any variation of the selenium precursors.

4.2. Optimization of the preparation parameters

The highest oxygen-reduction activity was observed for the catalysts made from selenious acid. In order to optimize the procedure of Method III, the heat-treatment temperature after the addition of selenium and the selenium content were selected as the operational parameters of the preparation.

The selected heat-treatment region is 250–350 °C, where critical changes happen in both ruthenium and selenium species. From the viewpoint of ruthenium, the level of crystallinity increases with temperature, as seen clearly in Figs. 1 and 3. The particle size increases slightly with temperature in this temperature region. A change in the selenium species is also distinct, as shown in the XP spectra (Fig. 6). In the Se 3d spectrum of the RuSe/C calcined at 250 °C, the high-binding-energy peak representing the selenium species in a high oxidation state is much stronger than the peak representing the zero-valence selenium species. A large amount of selenium in a high oxidation state is present in this catalyst because selenious acid is not completely reduced at 250 °C. The amount of elemental selenium or selenium interacting with ruthenium rises at 300 °C, reaching a very similar amount of high-oxidation-state selenium. This trend continues for the catalyst calcined at 350 °C. The performance of the catalyst calcined at 300 °C is considerably improved compared with that calcined at 250 °C as a result of the decomposition of selenious acid. The decrease of the performance at 350 °C is due to the agglomeration of the ruthenium particles.

The selenium content also affects the oxygen-reduction activity (see Fig. 9). However, the extent of this influence is relatively small compared with that of the calcination temperature. The heat-treatment procedure brings about a loss of selenium, but the higher nominal concentration may leave a larger amount of actual selenium after calcination until the site for selenium on the ruthenium surface is saturated. With increasing nominal selenium content, the oxygen-reduction activity is increased by the enhanced formation of the active phase. The selenium content does not influence the particle size distribution in the cases of both selenious acid and elemental selenium (see Fig. 4).

5. Conclusions

Based on the above experimental observations and discussion, we may draw the following conclusions about the effect of the RuSe/C preparation method on its catalytic oxygen-reduction behavior. The inorganic precursor methods show higher oxygen-reduction activity than the carbonyl method as a result of the higher dispersion of the ruthenium particles and enhanced formation of the active phase. Selenious acid is a better material for the inorganic precursor method than elemental selenium. The heat-treatment temperature has a great influence on the performance of the catalysts prepared by the inorganic precursor method. The optimum temperature is 300 °C from the viewpoint of active species formation and particle size distribution. The maximum power density achieved with 80 wt.% RuSe/C is 62 mW cm^{-2}.

References

[1] S. Ye, A. Vijh, L. Dao, J. Electroanal. Chem. 415 (1996) 115–121.
[2] J. Fournier, G. Faubert, J.Y. Tilquin, R. Cote, D. Guay, J.P. Dodelet, J. Electrochem. Soc. 144 (1997) 145–154.
[3] M. Lefevre, J.P. Dodelet, P. Bertrand, J. Phys. Chem. B 106 (2002) 8705–8713.
[4] S. Baranton, C. Coutanceau, C. Roux, F. Hahn, J.-M. Leger, J. Electroanal. Chem. 577 (2005) 223–234.
[5] A.J. Wagner, G.M. Wolfe, D.H. Fairbrother, Appl. Surf. Sci. 219 (2003) 317–328.
[6] P.H. Matter, L. Zhang, U.S. Ozkan, J. Catal. 239 (2006) 83–96.
[7] N. Alonso-Vante, W. Jaegermann, H. Tributsch, W. Honle, K. Yvon, J. Am. Chem. Soc. 109 (1987) 3251–3257.
[8] A.K. Shukla, R.K. Raman, Annu. Rev. Mater. Res. 33 (2003) 155–168.
[9] N. Alonso-Vante, H. Tributsch, O. Solorza-Feria, Electrochim. Acta 40 (1995) 567–576.
[10] M. Bron, P. Bogdanoff, S. Fiechter, I. Dorbandt, M. Hilgendorff, H. Schulenburg, H. Tributsch, J. Electroanal. Chem. 500 (2001) 510–517.
[11] N. Alonso-Vante, M. Fieber-Erdmann, H. Rossner, E. Holub Krappe, Ch. Giorgetti, A. Tadjeddine, E. Dartyge, A. Fontaine, R. Frahm, J. Phys. IV France 7 (1997) 887–890, C2.
[12] V.I. Zaikovskii, K.S. Nagabhushana, V.V. Kriventsov, K.N. Loponov, S.V. Cherepanova, R.I. Kvon, H. Bönnemann, D.I. Kochubey, E.R. Savinova, J. Phys. Chem. B 110 (2006) 6881–6890.
[13] M. Hilgendorff, K. Diesner, H. Schulenburg, P. Bogdanoff, M. Bron, S. Fiechter, J. New Mater. Electrochem. Syst. 5 (2002) 71–81.
[14] H. Schulenburg, M. Hilgendorff, I. Dorbandt, J. Radnik, P. Bogdanoff, S. Fiechter, M. Bron, H. Tributsch, J. Power Sources 155 (2006) 47–51.
[15] J.F. Moulder, W.F. Stickle, P.E. Sobol, K.E. Bomben, Handbook of X-ray Photoelectron Spectroscopy, Physical Electronics Inc., Minnesota, 1979, pp. 96–97.
[16] L. Zhang, J. Zhang, D.P. Wilkinson, H. Wang, J. Power Sources 156 (2006) 171–182.
[17] H.S. Wroblova, Y.C. Pan, G. Razumney, J. Electroanal. Chem. 69 (1976) 195–201.